

GAZİ

JOURNAL OF ENGINEERING SCIENCES

Evaluation of Different Mesh Types of Steel Roof Trusses According to AISC360-16 Code

Hilmi Arisoy^a, Gunnur Yavuz^b

Submitted: 17.01.2023 Revised: 28.04.2023 Accepted: 30.05.2023 doi:10.30855/gmbd.0705070

ABSTRACT

Keywords: Steel structure, industrial building, roof truss, AISC 360-16, LRFD

^{a,*} Konya Technical University,
Faculty of Engineering and Natural
Sciences,
Dept. of Civil Engineering
42250 - Konya, Türkiye
Orcid: 0000-0002-1436-0539
e mail: harisoy@ktun.edu.tr

^b Konya Technical University,
Faculty of Engineering and Natural
Sciences,
Dept. of Civil Engineering
42250 - Konya, Türkiye
Orcid: 0000-0002-8725-7129
e mail: gyavuz@ktun.edu.tr

*Corresponding author:
harisoy@ktun.edu.tr

Steel roof trusses are a frequently used element for carrying roof cover in industrial type structures. Roof trusses are generally preferred for long spans that cannot be designed with standard sections. These load bearing members can be created using many different types of mesh. In recent years, it has been observed that there are damages in the steel roof trusses due to heavy snowfall, especially in industrial buildings. Therefore, it is important to design these members safely and economically. In this study, roof trusses with 24 m span, 0.8 m side and 3.2 m ridge height were investigated for 5 different mesh types. A total of 20 analyses were performed for 4 different purlin distances using the SAP2000 program. Specification for Structural Steel Buildings (AISC 360-16) published by The American Institute of Steel Construction was used for the member design of these 20 roof trusses, whose external geometric dimensions are the same. As a result, the most economical roof truss type and purlin distance were determined by comparing the roof truss and roof truss + purlin weights obtained from the design. Minimum cross sections and minimum total weight were obtained for Warren truss mesh type with 2.4 m purlin distance.

Farklı Örgü Tiplerindeki Çelik Çatı Makaslarının AISC360-16 Yönetmeliğine Göre Değerlendirilmesi

ÖZ

Çelik çatı makasları, endüstriyel yapılarda çatı örtüsünü taşımak için yaygın olarak kullanılan taşıyıcı sistem elemanlarıdır. Çatı makasları genellikle standart kesitlerle tasarlanamayan uzun açıklıklar için tercih edilmektedir. Bu taşıyıcı elemanları oluşturmak için birçok farklı örgü türü kullanılmaktadır. Son yıllarda özellikle endüstriyel binalarda yoğun kar yağışı nedeniyle çelik çatı makaslarında hasarlar olduğu gözlemlenmektedir. Bu nedenle, bu elemanların güvenli ve ekonomik bir şekilde tasarlanması önem arz etmektedir. Bu çalışmada, 5 farklı örgü tipi için 24 m açıklıklı, 0.8 m kenar ve 3.2 m mahya yüksekliğine sahip çatı makasları incelenmiştir. SAP2000 programı kullanılarak 4 farklı aşık aralığı için toplam 20 adet analiz yapılmıştır. Dış geometrik ölçüleri aynı olan bu 20 adet çatı kirişine ait elemanların tasarımında Amerikan Çelik Konstrüksiyon Enstitüsü tarafından yayımlanan Yapısal Çelik Binalar Yönetmeliği (AISC 360-16) kullanılmıştır. Sonuç olarak, tasarımdan elde edilen çatı makası ve çatı makası + aşık ağırlıkları karşılaştırılarak en ekonomik çatı makası tipi ve aşık aralığı belirlenmiştir. En küçük kesitler ve en küçük toplam ağırlık Warren kafes tipi çatı makasında 2.4 m aşık aralığı için elde edilmiştir.

Anahtar Kelimeler: Çelik yapılar, endüstriyel binalar, çatı makası, AISC 360-16, YDKT

1. Introduction

The beams designed to carry the roof covering in steel structures are called roof beams. These beams carry the weight of the roof covering and the loads acting on this member. Roof beams can be designed using standard sections for short spans. The dominant internal force in the design of roof beams is usually the bending moment. As the span increases, the bending moment formed in the beam also increases. One of the most ideal ways to meet this moment demand is to increase the beam height. Together with the bending moment, the shear force also occurs in the beam. However, the shear force capacity of the beam is usually quite higher than the demand. When the moment capacity is increased by increasing the beam height, the beam web cannot be used effectively. For this reason, designs with standard cross-sections do not give economical results for long spans. Industrial buildings usually need large openings for a well-planned work area. At this point, roof trusses are used instead of standard sections. Roof trusses are obtained by joining the ends of the members at the joints. The elements used in the roof truss do not transfer moment to the joints. Therefore, only axial force occurs on the elements of a roof truss, which is loaded from the joints. The members utilized as a part of steel truss framework are generally angles, double angles, channels, double channels, square hollow sections and circle hollow sections [1].

The roof truss mesh can be created in many different types. Warren truss, Howe truss and Pratt truss are the most common types of trusses [2]. These types have been used in trusses for many years. Before the widespread use of steel, roof trusses were usually made of wood [3]. Since the use of wooden roof trusses, the designs of different types of roof trusses have been studied. Nowadays, optimization plays a big role in the design of structures with a long span [4]. It is aimed to design roof trusses safely and economically by using optimization techniques. Considering the size of the areas where roof trusses are used, a small improvement in the design will make a great contribution economically. However, mistakes made in this design will have very severe consequences. The cost of damage caused by excessive snow load should be considered not only as repair costs, but also as the inability to use the building for a while, damage to the materials inside the building, possible injuries and loss of life [5]. When the published reports on the damaged steel roof trusses are examined, it was concluded that one of the biggest factors is the snow load [6]. It is observed that many steel roof trusses have collapsed due to heavy snowfall in the past. In this study, it is aimed to determine which of the roof trusses with different mesh types are the most economical for situations where snow load is the dominant load in the design.

2. Analysis of Different Roof Truss Types

In this study, the effect of mesh types for a steel roof truss was analysed. The examined roof trusses have a span of 24 m, a side height of 0.8 m and a ridge height of 3.2 m (Figure 1). In this design, the mesh type and purlin distance parameters are selected as variable. A total of 20 analyses were performed for 4 different purlin distances and 5 different mesh types.

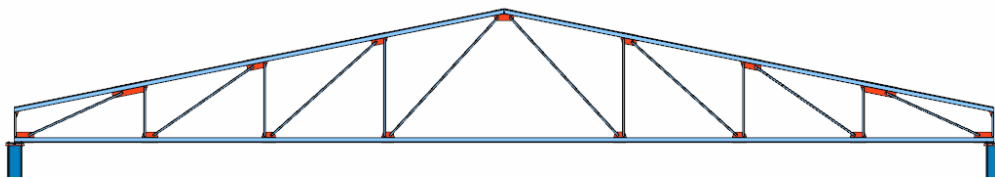


Figure 1. 3D view of T1 type roof truss

The five different mesh types used in the study are shown in Figure 2. T1, T2 and T3 types were chosen as the Howe, Pratt and Warren truss types, respectively, which are often used. T4 and T5 types were also created as a combination of other types. Since the roof truss can only be loaded from the joints, each type of mesh is arranged for purlin distance of 3.0 m, 2.4 m, 2.0 m and 1.5 m. The models created according to different purlin distances for the T1 mesh type are shown in Figure 3 as an example.

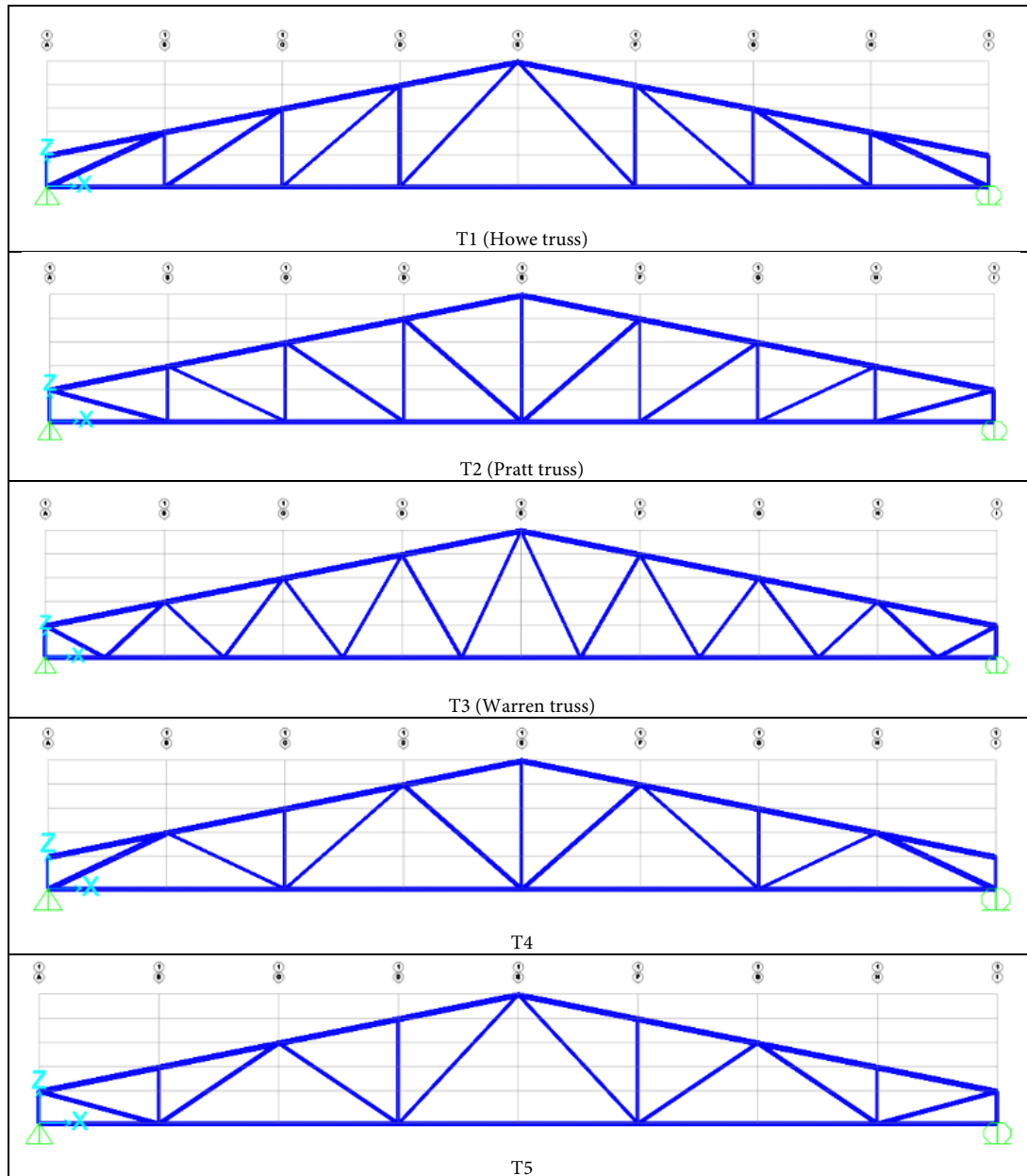


Figure 2. Roof truss types

The analyses were performed using SAP2000 v23.0 structural analysis and design program [7]. The steel grade of the profiles to be used in the steel roof truss has been selected as S235 defined in TS EN 10025-2 [8]. S235 grade steel has 235 MPa yield strength and 360 MPa tensile strength.

This study was carried out for the case when the snow load is effective in the design. For this reason, only the dead load (D) and snow load (S) are taken into account in the design. Other loads such as earthquake load, wind load, ice load and storm load have been ignored. The design was made in accordance with the Load and Resistance Factor Design (LRFD) provision. The following load combinations were obtained using ASCE/SEI 7-16 [9].

Load combinations for the limit states of strength;

- 1.4 D
- 1.2 D + 0.5 S
- 1.2 D + 1.6 S

Load combinations for the limit states of serviceability;

- 1.0 D + 0.5 S

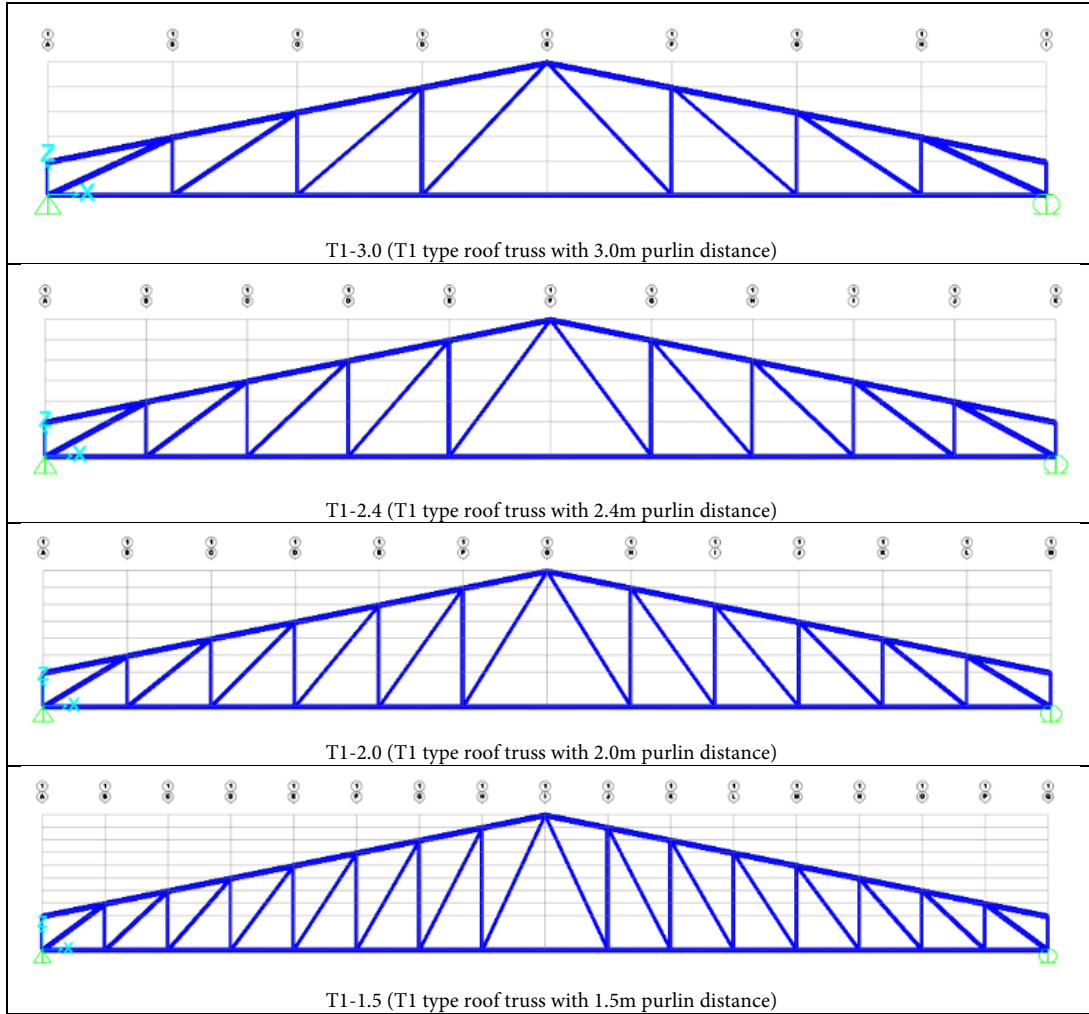


Figure 3. T1 type roof trusses with different purlin distances

The double angle built-up section was used for designing tension and compression members of roof trusses. A typical double angle section is shown in Figure 4. Also, all double angle sections used in steel design are given in Table 1.

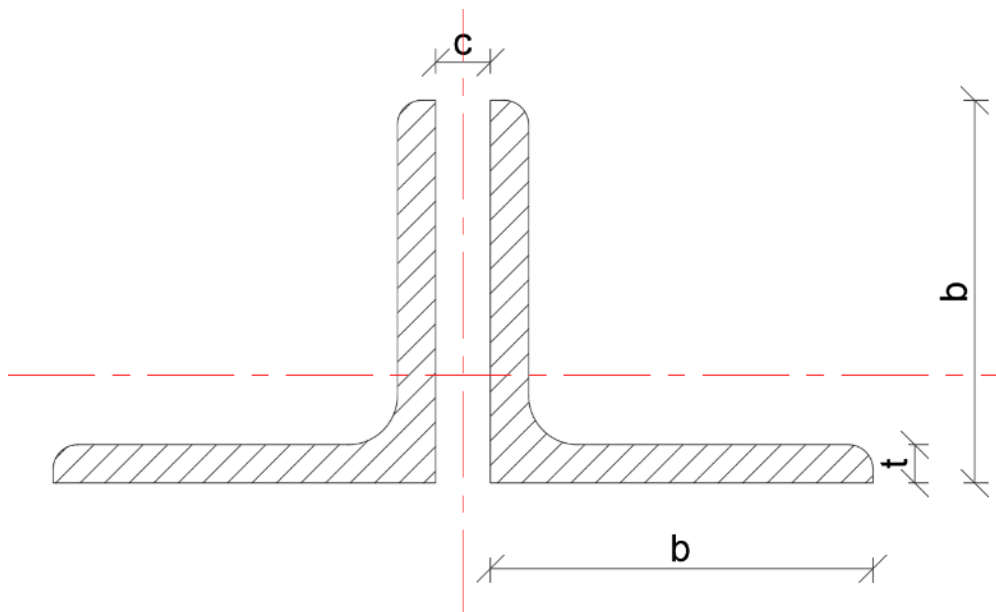


Figure 4. Typical double angle section ($2LbXt/c$)

Table 1. Steel section list used in the design

Section list	
2L45X4.5/10/	2L75X7/10/
2L50X5/10/	2L80X8/10/
2L55X5/10/	2L90X9/10/
2L60X6/10/	2L100X10/10/
2L65X6/10/	2L110X10/10/
2L70X7/10/	2L120X12/10/

One end of the roof trusses was modeled as a pinned support and the other end as a roller support. Also, pinned connections were defined at the ends of the members. The weight of the roof trusses was automatically added to the dead load. In addition, a dead load of 0.1 kN/m² on the roof was taken into account. The characteristic snow load value was determined as 1.60 kN/m² from TS EN 1991-1-3 [10]. The distance between the roof trusses was considered to be 7.5 m. The individual loads at the joints were calculated by the loads spread over the area were multiplied by the purlin distance and 7.5 m. The snow load values calculated for T1-3.0 roof truss are shown in Figure 5 as an example.

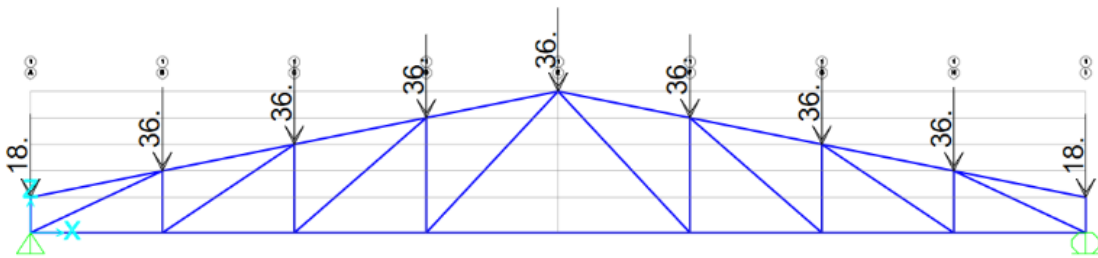


Figure 5. Snow load for T1-3.0 (kN)

The axial force values of the members found as a result of the analysis are shown in Figure 6, and the deformed roof truss shape is shown in Figure 7 for T1-3.0 roof truss.

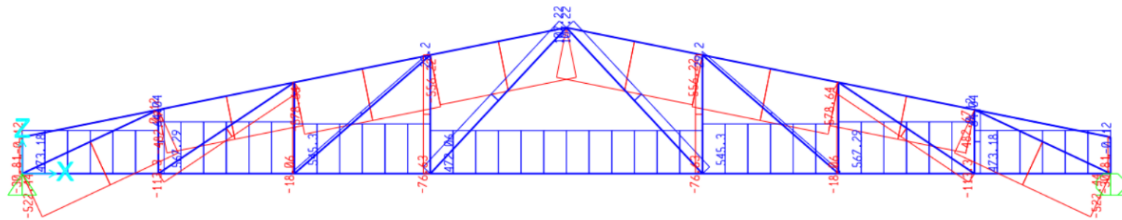


Figure 6. Axial force diagram for T1-3.0 (kN)

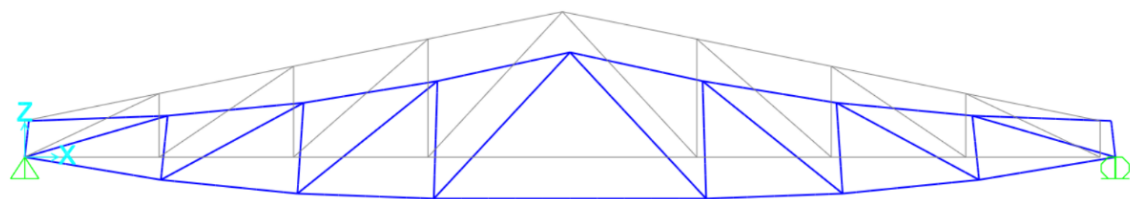


Figure 7. Deformed shape for T1-3.0

In the SAP2000 program, the analyses were performed in the two dimensions. The design of steel elements was made using the AISI 360-16 regulation [11]. When designing the tension members, the limit states of tensile yielding in the gross section and tensile rupture in the net section were taken into account using Equation 1 and Equation 2, respectively. It was assumed that the effective net area to gross area ratio of members is 0.8. In addition, the limit value of 300 which is recommended by the regulation was used for the slenderness of the tension members.

$$P_{nt} = F_y * A_g \quad (\text{the limit state of tensile yielding}) \quad (1)$$

$$P_{nt} = F_u * A_e \quad (\text{the limit state of tensile rupture}) \quad (2)$$

Where; P_n : characteristic tensile strength, F_y : yield stress, F_u : tensile stress, A_g : gross area of a section, A_e : effective section area which can be calculated by $A_n * U$ (U : shear lag factor, A_n : net section area)

The limit states of flexural buckling and flexural-torsional buckling were taken into account when designing the compression members by Equations 3 to 7. All the sections given in Table 1 are classified as nonslender-element sections according to AISC360-16 Table B4.1a. For this reason, local buckling does not occur in the compression members. In addition to the strength of these elements, it was checked that the slenderness did not exceed the maximum permissible value of 200. In these elements, since the both ends of the elements are connected with pinned support, the effective length factor is taken as 1. For built-up sections, it is necessary to calculate the modified slenderness value depending on the type and placement of the fasteners. In this study, the fasteners were not calculated. Therefore, it was assumed that the modified slenderness ratio of the members was 1.1 times the slenderness ratio of the corresponding member. The same cross-section was selected to the complete top chord elements when designing. Similarly, the all bottom chord elements were designed with the same cross-section. The design results for the T1-3.0 roof truss are shown in Figure 8.

$$P_{nc} = F_{cr} * A_g \quad (\text{the limit state of buckling}) \quad (3)$$

$$\text{When } \frac{F_y}{F_e} \leq 2.25 \quad F_{cr} = \left(0.658 \frac{F_y}{F_e}\right) F_y \quad (4)$$

$$\text{When } \frac{F_y}{F_e} > 2.25 \quad F_{cr} = 0.877 F_e \quad (5)$$

$$F_e = \frac{\pi^2 E}{\left(\frac{L_c}{r}\right)^2} \quad (\text{for flexural buckling}) \quad (6)$$

$$F_e = \left(\frac{F_{ey} + F_{ez}}{2H}\right) \left[1 - \sqrt{1 - \frac{4F_{ey}F_{ez}H}{(F_{ey} + F_{ez})^2}}\right] \quad (\text{for flexural-torsional buckling}) \quad (7)$$

Where; P_n : characteristic compression strength, F_y : yield stress, F_e : elastic buckling stress, F_{ey} : elastic buckling stress about y-axis, F_{ez} : elastic buckling stress about longitudinal axis, F_{cr} : critical stress, A_g : gross area of a section, L_c : effective length of member for buckling, E : modulus of elasticity of steel (200000 MPa), r : radius of gyration, H : flexural constant.

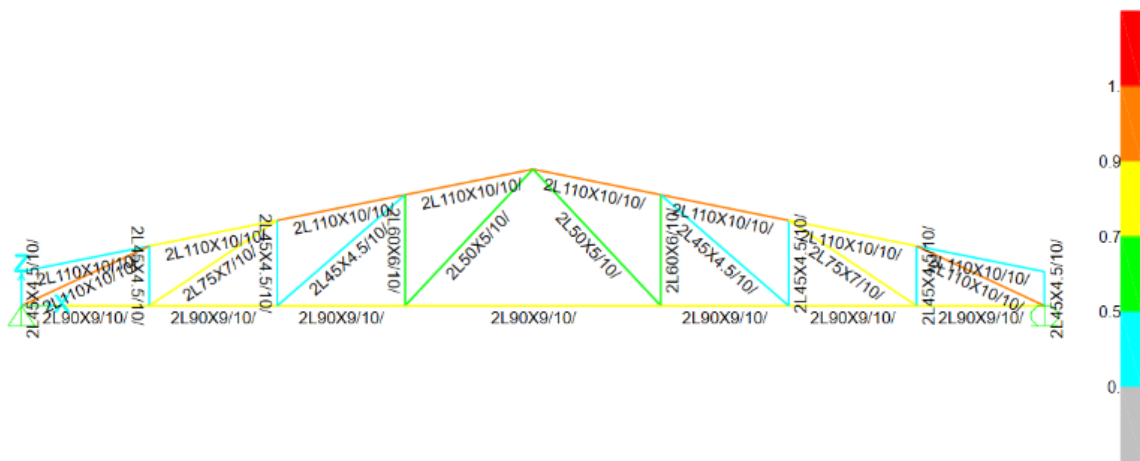


Figure 8. Design sections and capacity ratios for T1-3.0

In addition to the roof truss, the design of purlins was also made. The purlins were solved as a singular element independently of the roof truss (Figure 9). One end of the purlins is designed as a pinned support, the other end is designed as a roller support. The purlins are designed to have a sag rod at the $L/3$ points (L : beam span). For this reason, the displacement in the horizontal direction is restricted at $L/3$ points.

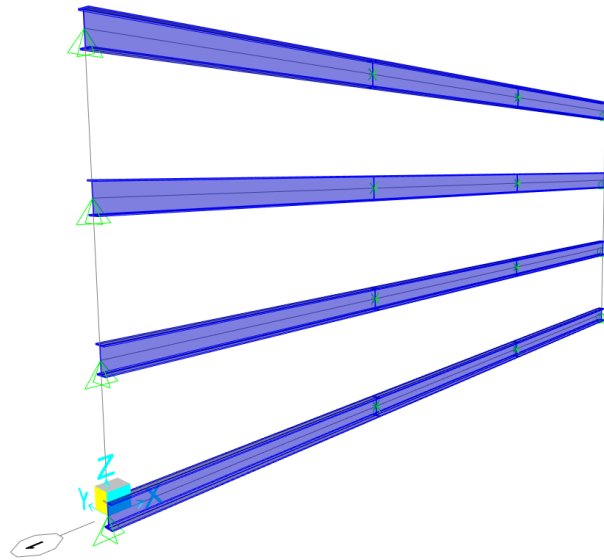


Figure 9. 3D view of purlins

The snow load was added on the purlins as a linear distributed load (Figure 10). The purlins standing on the roof truss have the effect of bending in both directions due to the slope of the roof truss. Linear distributed loads were obtained by multiplying the purlin distance with the snow load acting on the unit area. The loads found were distributed in 2 directions according to the slope of the roof truss. The obtained bending moment graphs are given in Figure 11.

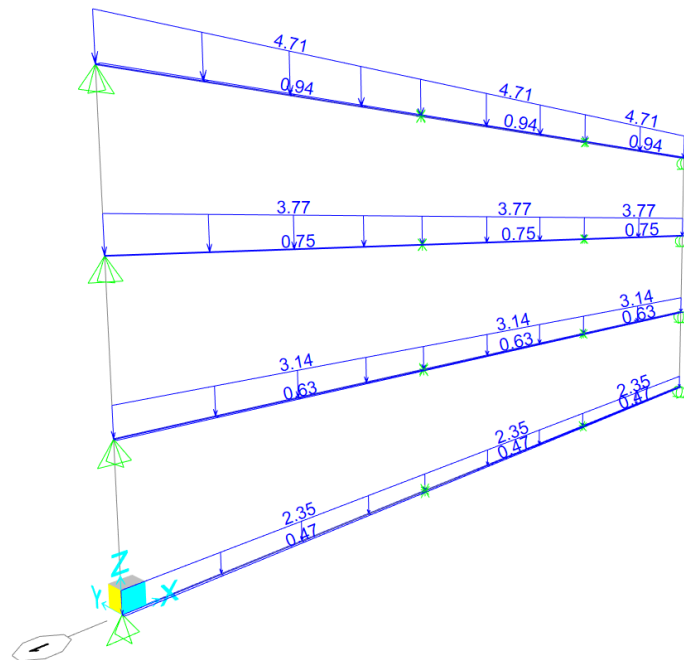
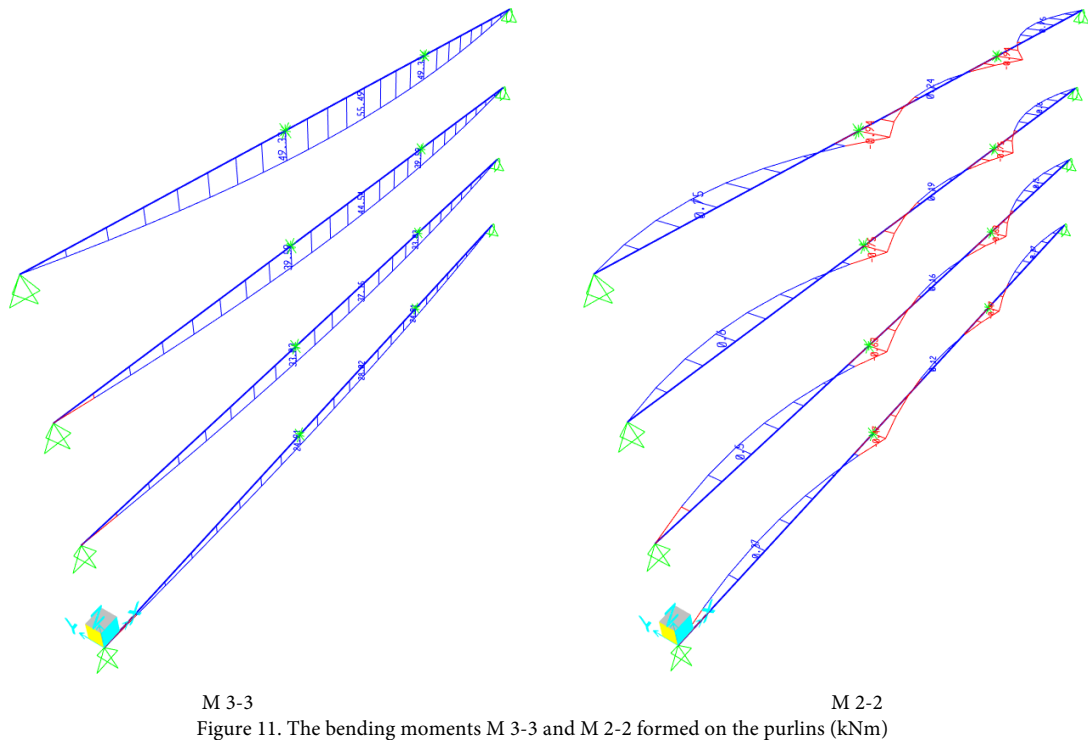


Figure 10. Snow load for the purlins (kN/m)

Purlins are designed under the effect of two-way bending moment and shear force. IPE sections were used for the purlins. Since all cross-sections used in the purlins are compact, the design was made by considering the limit state of yielding and the limit state of lateral torsional buckling for bending about major axis using Equation 8 to 11. Similarly, for bending about minor axis, the limit state of yielding was taken into account by Equation 12. The capacity ratios of purlins under the effect of two-way bending moment are shown in Figure 12. For the shear force, the design was made using Equation 13 and Equation 14 in the strong and weak direction, respectively. Also, the capacity ratios for shear forces in both directions are given in Figure 13.



M 3-3 M 2-2
Figure 11. The bending moments M 3-3 and M 2-2 formed on the purlins (kNm)

$$M_n = M_p = F_y W_{px} \quad (\text{the limit state of yielding}) \quad (8)$$

$$\text{For } L_b \leq L_p \quad (\text{the limit state of lateral-torsional buckling does not apply}) \quad (9)$$

$$\text{For } L_p < L_b \leq L_r \quad M_n = C_b \left[M_p - (M_p - 0.7 F_y W_{ex}) \left(\frac{L_b - L_p}{L_r - L_p} \right) \right] \leq M_p \quad (10)$$

$$\text{For } L_b > L_p \quad M_n = F_{cr} W_{ex} \quad (11)$$

$$M_n = M_p = F_y W_{py} < 1.6 F_y W_{ey} \quad (\text{the limit state of yielding}) \quad (12)$$

$$V_n = 0.6 F_y A_w C_{v1} \quad (13)$$

$$V_n = 0.6 F_y b_f t_f C_{v2} \quad (14)$$

Where; M_n : characteristic flexural strength, M_p : plastic flexural strength, W_{px} : plastic section modulus about the x-axis, W_{ex} : elastic section modulus about the x-axis, W_{py} : plastic section modulus about the y-axis, W_{ey} : elastic section modulus about the y-axis, C_b : lateral-torsional buckling modification factor, F_{cr} : critical stress for lateral-torsional buckling L_b : length between points that are either braced against lateral displacement of the compression flange or braced against twist of the cross section, L_p : the limiting laterally unbraced length for the limit state of yielding, L_r : the limiting unbraced length for the limit state of inelastic lateral-torsional buckling, A_w : area of web, C_{v1} and C_{v2} : the web shear strength coefficients, b_f : width of flange, t_f : thickness of flange.

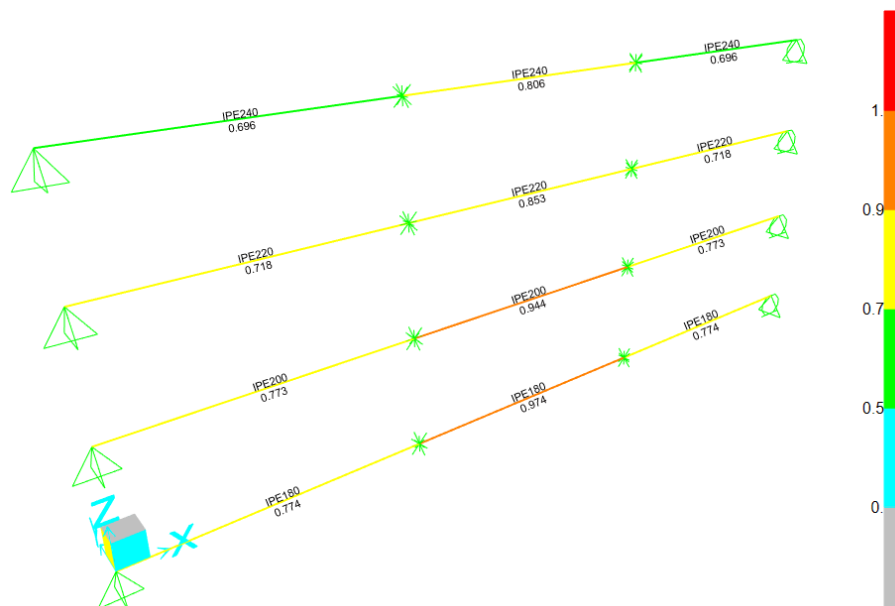


Figure 12. Capacity ratios of purlins for bending moments

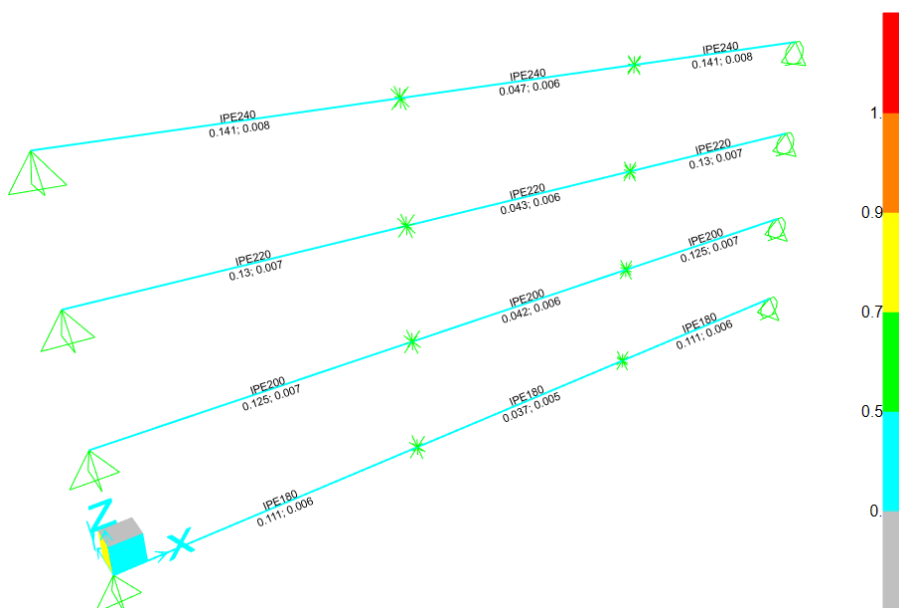


Figure 13. Capacity ratios of purlins for shear force

3. Comparison of Analysis Results

The roof truss weights obtained as a result of the analysis are given in Table 2. Also, the obtained data are shown in Figure 14 as a surface plot. The lowest roof truss weight was achieved for the T3 (Warren) type at a purlin distance of 2.4 m. Table 3 shows how much the roof truss weights are higher than the lowest roof truss weight by percentage.

Table 2. Roof truss weights (kN)

Purlin distance (m)	Roof truss type					Avg.
	T1	T2	T3	T4	T5	
3.0	19.17	18.40	17.34	18.56	18.18	18.33
2.4	18.24	17.70	16.86*	17.52	17.35	17.53
2.0	18.27	17.97	17.22	17.54	17.13	17.63
1.5	18.95	18.66	18.08	17.95	17.59	18.25
Avg.	18.66	18.18	17.38	17.89	17.56	

*Minimum weight

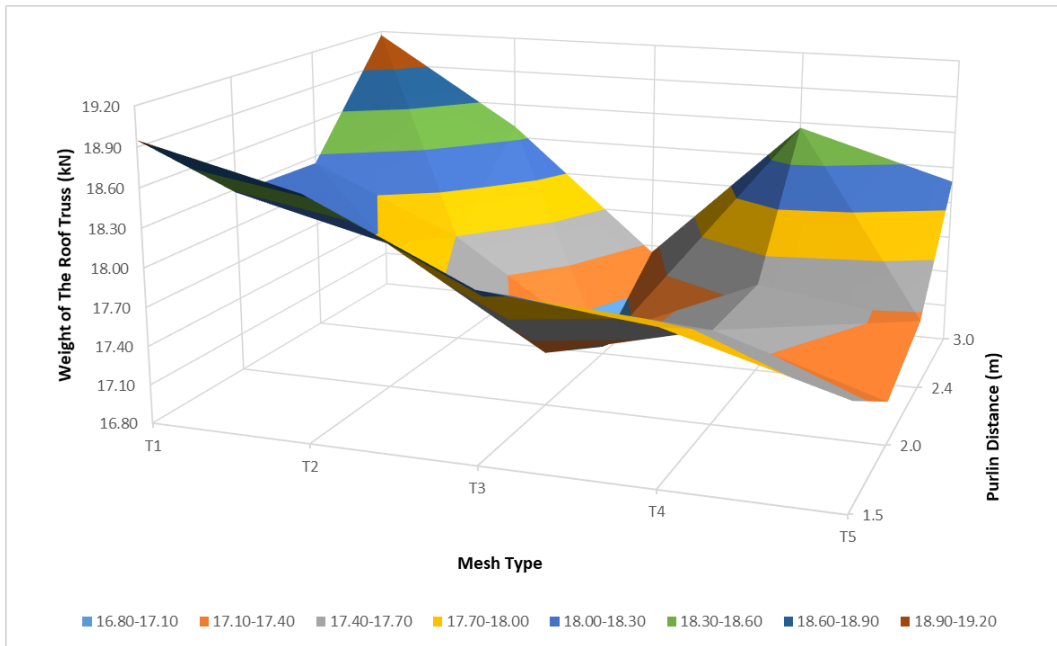


Figure 14. Surface plot of truss weight

Table 3. Percentage difference according to the minimum roof truss weights (%)

Purlin distance (m)	Roof truss type				
	T1	T2	T3	T4	T5
3.0	13.68	9.13	2.85	10.06	7.83
2.4	8.19	4.96	0.00	3.93	2.91
2.0	8.38	6.58	2.13	4.01	1.61
1.5	12.41	10.66	7.25	6.47	4.32

When the comparison was made according to the type of mesh, the weights of the roof trusses from the lowest to the highest were obtained as follows (Figure 15);

$$W_{T3} < W_{T5} < W_{T4} < W_{T2} < W_{T1}$$

In this comparison, the same ranking was obtained for the average values and the minimum values.

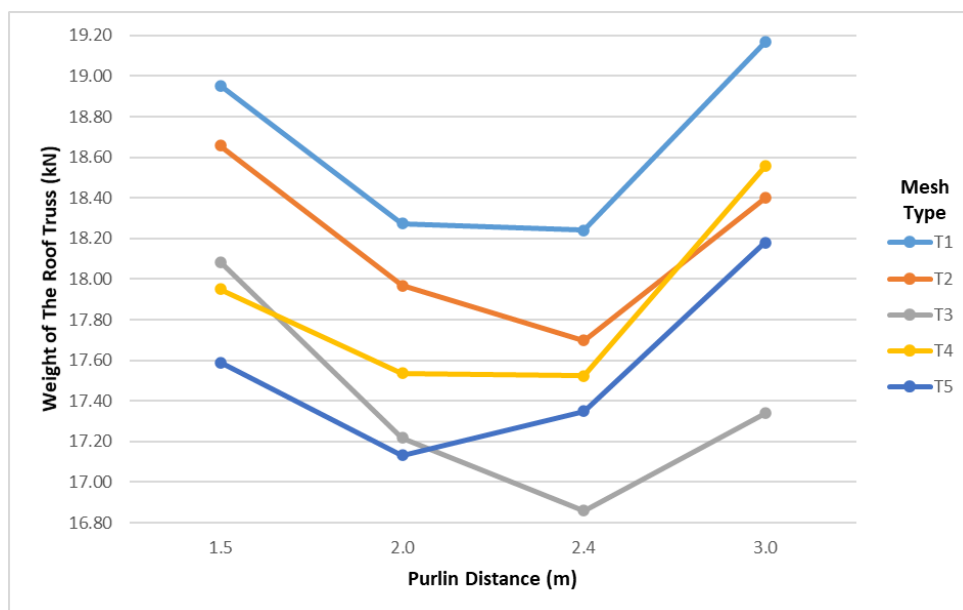


Figure 15. Truss weights vs mesh types

When the roof truss weights are evaluated according to the purlin distance, the following ranking has been

obtained (Figure 16).

for the average roof truss weights;

$$W_{2.4} < W_{2.0} < W_{1.5} < W_{3.0}$$

for the minimum roof truss weights;

$$W_{2.4} < W_{2.0} < W_{3.0} < W_{1.5}$$

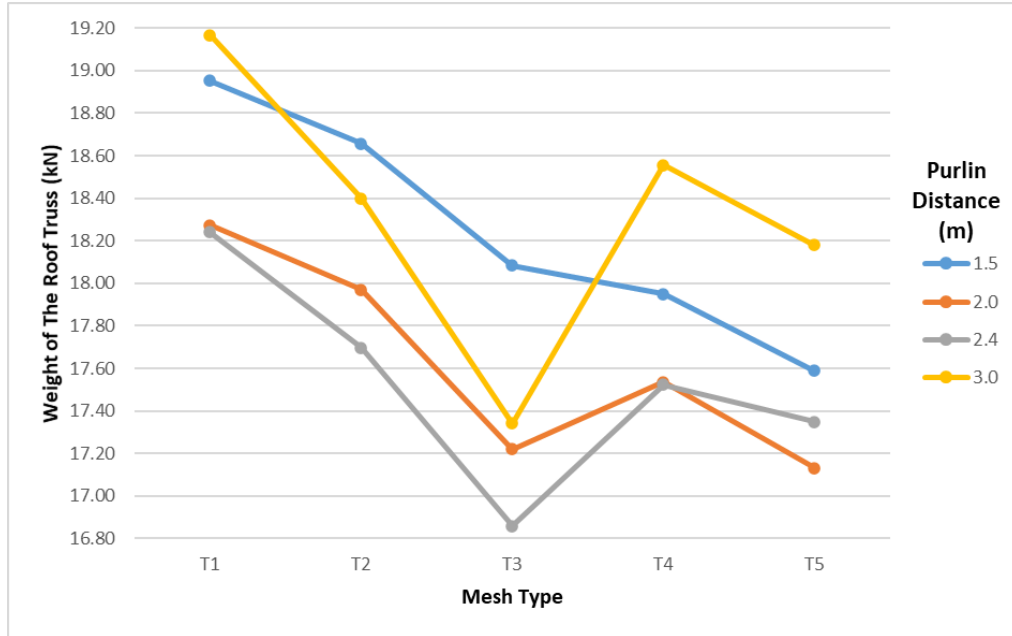


Figure 16. Truss weights vs purlin distances

The displacements at the midpoint of the roof trusses are shown in Table 4. The maximum allowable displacement is calculated as 80 mm using the limit value of $L/300$ [9]. All the displacement values obtained are less than this limit value.

Table 4. Displacements at the midpoint of the roof trusses (mm)

Purlin distance (m)	Roof truss type				
	T1	T2	T3	T4	T5
3.0	22.34	23.57	21.79	22.45	22.99
2.4	22.76	23.99	22.74	23.11	23.05
2.0	22.89	23.83	22.73	22.75	23.21
1.5	22.78	23.62	23.02	22.39	22.94

As a result of the analysis of the purlins, the purlin sections were obtained as shown in the Table 5. The weight of a purlin with a length of 7.5 m for each section is indicated in the third column of Table 5. For each purlin distance, the total number of purlins between two roof trusses and, accordingly, the total weight of the purlins were calculated.

Table 5. Cross sections and weights of the purlins

Purlin distance (m)	Purlin section	Purlin weight (kN)	Number of purlins	Total purlin weight (kN)
3.0	IPE 240	2.26	10	22.58
2.4	IPE 220	1.93	12	23.14
2.0	IPE 200	1.65	14	23.04
1.5	IPE 180	1.38	18	24.84

The total roof weight was obtained by collecting the purlin weights and the roof truss weights (Table 6). In addition, the percentage differences according to the minimum value are shown in Table 7.

Table 6. Total roof weights (kN)

Purlin distance (m)	Roof truss type					Avg.
	T1	T2	T3	T4	T5	
3.0	41.75	40.98	39.92*	41.14	40.76	40.91
2.4	41.38	40.83	40.00	40.66	40.49	40.67
2.0	41.32	41.01	40.26	40.58	40.18	40.67
1.5	43.79	43.50	42.92	42.79	42.43	43.09
Avg.	42.06	41.58	40.78	41.29	40.96	

*Minimum weight

Table 7. Percentage difference according to minimum total roof weights (%)

Purlin distance (m)	Roof truss type				
	T1	T2	T3	T4	T5
3.0	4.58	2.66	0.00	3.05	2.10
2.4	3.65	2.29	0.19	1.85	1.42
2.0	3.50	2.74	0.86	1.65	0.64
1.5	9.70	8.96	7.52	7.19	6.28

With the addition of purlin weights, it is seen that the order given for the mesh type remains the same (Figure 17);

$$W_{T3} < W_{T5} < W_{T4} < W_{T2} < W_{T1}$$

However, with the addition of purlin weights, it is seen that the order given for the purlin distance changes as follows (Figure 18);

for the average roof truss weights;

$$W_{2.4} = W_{2.0} < W_{3.0} < W_{1.5}$$

for the minimum roof truss weights;

$$W_{3.0} < W_{2.4} < W_{2.0} < W_{1.5}$$

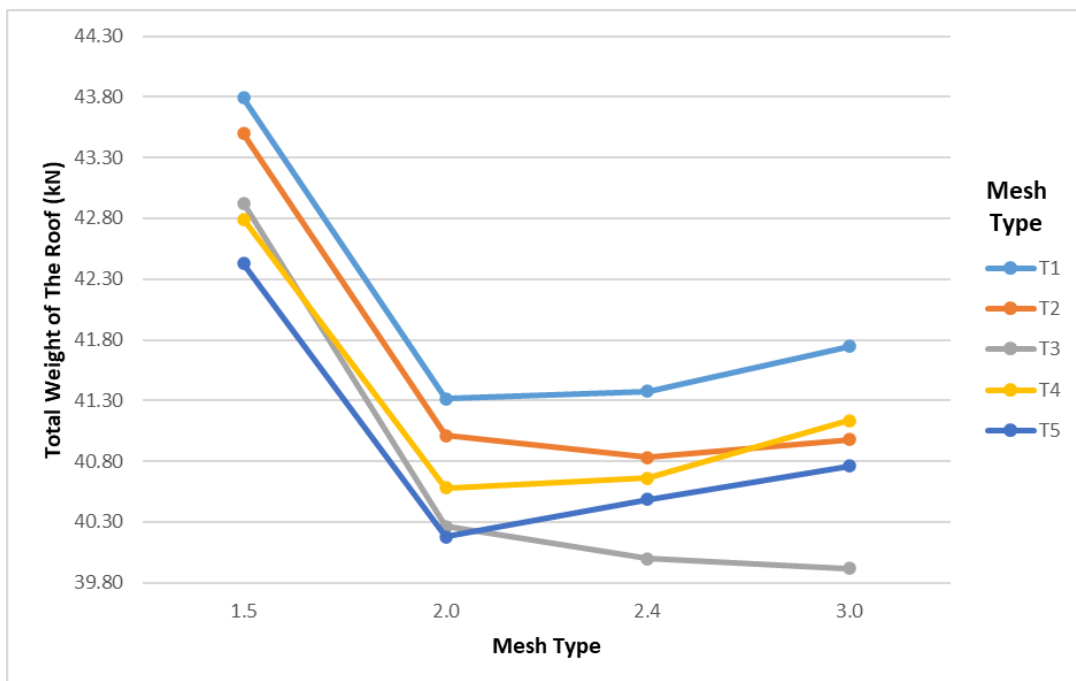


Figure 17. Total roof weights vs mesh types

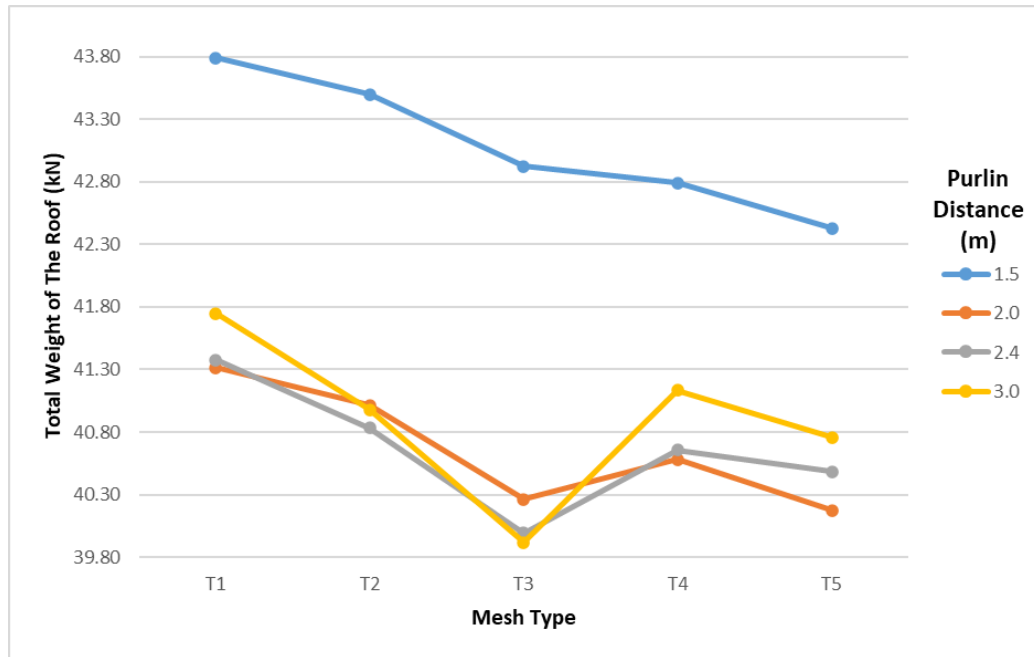


Figure 18. Total roof weights vs purlin distances

4. Results and Discussion

Many steel roofs have been damaged due to heavy snowfalls experienced in recent years. These damages have led to great financial losses. In order to prevent these losses, a design should be made that has both sufficient strength and is economical. For this reason, this study has been carried out in order to provide convenience to those who want to design a steel roof. In this study, the effect of mesh type and purlin distance on the weight of steel roof trusses was investigated in the case where snow load is the dominant load. The results obtained from this study are limited to the cases where only the snow load is effective in the design. Some important results of this study can be summarized as follows:

- The most economical result among the types of roof truss mesh is obtained from the T3 (Warren) type with 3.0 m purlin distance.
- In the weight of the steel roof, the roof trusses and the purlins have approximately the same proportion of impact.
- For purlin distances below 2 m, the T5 type works better than the T3 type.
- The low truss weights have been achieved for the purlin distances of 2.0 m - 2.4 m. Although, an increase in total purlin weight was observed with a decrease in purlin distance. As a result, the minimum values for the total roof weight were obtained between 2.0 m - 3.0 m.
- The biggest roof truss weights were obtained from the T1 type. Similarly, the 1.5 m purlin distance has also led to obtaining the biggest roof weights.
- Similar displacement values were obtained for all roof trusses.

Conflict of Interest Statement

No potential conflict of interest was reported by the authors.

References

- [1] G. Kaur, R. S. Bansal and S. Kumar, "Shape Optimization of Roof Truss," *International Journal of Engineering Research & Technology (IJERT)*, vol. 5, pp. 696-700, 2016.
- [2] S. N. Rahane and S. K. Nalawade, "A Review on Optimization of Industrial Trusses," *International Journal of Research in Engineering, Science and Management*, vol. 5, no. 1, pp. 237-242, January 2022.
- [3] P. Munafò, F. Stazi, C. Tassi and F. Davi, "Experimentation on historic timber trusses to identify repair techniques compliant with the original structural-constructive conception," *Construction and Building Materials*, vol. 87, pp. 54-66, July 2015.

doi:10.1016/j.conbuildmat.2015.03.086

[4] Y. Shved, Y. Kovalchuk, L. Bodrova, H. Kramar and N. Shynhera, "Material consumption optimization of a welded rafter truss made of angle profiles," *Procedia Structural Integrity*, vol. 36, pp. 10-16, 2022. doi:10.1016/j.prostr.2021.12.076

[5] J. Geis, K. Strobel, and A. Liel, "Snow-induced building failures," *Journal of Performance of Constructed Facilities*, vol. 26, no. 4, pp. 377-388, August 2012. doi:10.1061/(ASCE)CF.1943-5509.0000222

[6] J. Krentowski, T. Chyzy, P. Dunaj, and P. Dunaj, "Delayed catastrophe of a steel roofing structure of a shopping facility," *Engineering Failure Analysis*, vol. 98, pp. 72-82, April 2019. doi:10.1016/j.engfailanal.2019.01.082

[7] CSI, "SAP2000 v23.0 Integrated Software for Structural Analysis and Design," Computers and Structures Inc., Berkeley, California, 2021.

[8] TSE, "TS EN 10025-2: Hot rolled products of structural steels. Part 2-Technical delivery conditions for non-alloy structural steels," Institute of Turkish Standard (TSE), Ankara, Türkiye, 2006.

[9] ASCE, "ASCE/SEI 7-16. Minimum Design Loads and Associated Criteria for Buildings and Other Structures – Provisions," ASCE Standard. American Society of Civil Engineers. 1801 Alexander Bell Drive, Reston, Virginia, 20191. ISBN 978-0-7844-1424-8, 2016.

[10] TSE, "TS EN 1991-1-3: Eurocode 1-Actions on structures-Part 1-3: General actions-Snow loads," Institute of Turkish Standard (TSE), Ankara, Türkiye, 2007.

[11] AISC, "ANSI/AISC 360-16: An American National Standard – Specification for Structural Steel Buildings," American Institute of Steel Construction. 130 East Randolph Street, Suite 2000, Chicago, Illinois, 60601. July 7, 2016

This is an open access article under the CC-BY license

